Advanced Composite Materials
Publication details, including instructions for authors and subscription information:
http://www.tandfonline.com/loi/tacm20

Rate-Dependence of Off-Axis Tensile Behavior of Cross-Ply: CFRP Laminates at Elevated Temperature and Its Simulation

Fumi Takeuchi [a], Masamichi Kawai [b], Jian-Qi Zhang [c] & Tetsuya Matsuda [d]

[a] Department of Engineering Mechanics and Energy, University of Tsukuba, Tsukuba 305-8573, Japan
[b] Department of Engineering Mechanics and Energy, University of Tsukuba, Tsukuba 305-8573, Japan;, Email: mkawai@kz.tsukuba.ac.jp
[c] Department of Engineering Mechanics and Energy, University of Tsukuba, Tsukuba 305-8573, Japan
[d] Department of Engineering Mechanics and Energy, University of Tsukuba, Tsukuba 305-8573, Japan
Version of record first published: 02 Apr 2012.

To cite this article: Fumi Takeuchi , Masamichi Kawai , Jian-Qi Zhang & Tetsuya Matsuda (2008): Rate-Dependence of Off-Axis Tensile Behavior of Cross-Ply: CFRP Laminates at Elevated Temperature and Its Simulation, Advanced Composite Materials, 17:1, 57-73

To link to this article: http://dx.doi.org/10.1163/156855108X295654

///VSP///

Advanced Composite Materials 17 (2008) 57–73

ADVANCED COMPOSITE MATERIALS
www.brill.nl/acm

Rate-Dependence of Off-Axis Tensile Behavior of Cross-Ply CFRP Laminates at Elevated Temperature and Its Simulation

Fumi Takeuchi, Masamichi Kawai *, Jian-Qi Zhang and Tetsuya Matsuda

Department of Engineering Mechanics and Energy, University of Tsukuba, Tsukuba 305-8573, Japan

Received 20 December 2006; accepted 27 March 2007

Abstract

The present paper focuses on experimental verification of the ply-by-ply basis inelastic analysis of multi-directional laminates. First of all, rate dependence of the tensile behavior of balanced symmetric cross-ply T800H/epoxy laminates with a $[0/90]_{3S}$ lay-up under off-axis loading conditions at 100°C is examined. Uniaxial tension tests are performed on plain coupon specimens with various fiber orientations $[\theta/(90-\theta)]_{3S}$ ($\theta = 0$, 5, 15, 45 and 90°) at two different strain rates (1.0 and 0.01%/min). The off-axis stress–strain curves exhibit marked nonlinearity for all the off-axis fiber orientations except for the on-axis fiber orientations $\theta = 0$ and 90°, regardless of the strain rates. Strain rate has significant influences not only on the off-axis flow stress in the regime of nonlinear response but also on the apparent off-axis elastic modulus in the regime of initial linear response. A macromechanical constitutive model based on a ply viscoplasticity model and the classical laminated plate theory is applied to predictions of the rate-dependent off-axis nonlinear behavior of the cross-ply CFRP laminate. The material constants involved by the ply viscoplasticity model are identified on the basis of the experimental results on the unidirectional laminate of the same carbon/epoxy system. It is demonstrated that good agreements between the predicted and observed results are obtained by taking account of the fiber rotation induced by deformation as well as the rate dependence of the initial Young's moduli.

Keywords

Polymer matrix composites, cross-ply laminate, off-axis loading, rate dependence, viscoplasticity, carbon fiber, epoxy, high temperature

1. Introduction

Deformation of glassy polymers depends on the time and rate of loading, and this tendency becomes stronger as temperature increases to the glass transition temperature [1–5]. This suggests that nonlinear deformation of unidirectional polymer

* To whom correspondence should be addressed. E-mail: mkawai@kz.tsukuba.ac.jp

Edited by the JSCM

DOI:10.1163/156855108X295654

matrix composites (PMCs) under off-axis loading conditions also exhibits significant time- and rate-dependence, especially at high temperatures, since the off-axis deformation of PMCs is controlled by the response of the matrix polymers employed. Therefore, characterization of the time- and rate-dependent nonlinear deformation of PMCs and establishment of an accurate rate-dependent constitutive model in a multiaxial form are prerequisite for designing reliable components and structures made of PMCs. These demands are crucial especially for the high-performance carbon fiber-reinforced polymer matrix composites (CFRPs) required by advanced aerospace structures which need to tolerate a range of temperature up to about 300°C [6, 7].

Effects of loading rate on the off-axis nonlinear stress–strain behavior of unidirectional CFRPs have been examined in several studies [8–10]. For example, Gates and Sun [8] examined the strain-rate dependence of the high-temperature tensile behavior of unidirectional AS4/PEEK laminates using off-axis coupon specimens. Kawai *et al*. [9] observed the high-temperature off-axis tensile behavior of similar unidirectional AS4/PEEK laminates under stress-controlled conditions and compared it with the response under strain-controlled conditions. In the studies by Sun and Yoon [10], effects of the change in strain rate on the off-axis tensile behavior of unidirectional AS4/PEEK laminates were elucidated, together with the influence of test temperature. It was also demonstrated in [9] that a permanent strain was caused by loading up to a relatively large stress level. These observations imply that the nonlinear rate-dependent deformation of those unidirectional CFRP laminates under off-axis loading features an inelastic part in some way analogous to viscoplasticity.

Macromechanical modeling of the rate-dependent nonlinear behavior of unidirectional CFRPs has been attempted by Sun and coworkers [8, 11, 12] and Ladeveze and Dantec [13]. Gates and Sun [8] extended the one-parameter plasticity model [14] and developed a viscoplasticity model based on the overstress concept. Yoon and Sun [11] proposed another plane–stress model; they extended the Bodner–Partom model [15] for viscoplastic behavior of isotropic materials with the help of the effective stress and inelastic strain defined by Sun and Chen [14]. Wang and Sun [12] elaborated the evolution equation of the scalar internal variable assumed in the Gates–Sun model. By comparison with experimental results, it has been shown that the Gates–Sun model [8], Yoon–Sun model [11] and Wang–Sun model [12] can adequately describe the rate-dependent nonlinear deformation of unidirectional PMC laminates under off-axis monotonic loading conditions. A similar plane–stress model was also developed by Ladeveze and Dantec [13], in which an effect of damage was further considered.

Most structural CFRPs are used in the form of multidirectional laminate in which unidirectional CFRP plies are stacked with different orientations. It is an interesting engineering approach that the time- and rate-dependent behavior of multidirectional CFRP laminates is analyzed on the basis of a viscoplasticity model for individual unidirectional plies. Such attempts have not sufficiently been made until quite re-

cently. In earlier studies [16, 17], it was shown that a ply-by-ply basis viscoplasticity approach succeeded in adequately predicting the overall creep and stress relaxation behaviors of symmetrical angle-ply CFRP laminates at high temperature.

In the present study, the ply-by-ply basis viscoplasticity approach is further tested for the off-axis deformation behavior of a symmetrical alternating cross-ply CFRP laminate under off-axis loading at different strain rates. First, monotonic tension tests are performed on off-axis plain coupon specimens at high temperature for different strain rates. Then, simulations are carried out using the constitutive model based on the classical laminated plate theory [18, 19] for composite homogenization and the viscoplasticity model of a modified Gates–Sun type for individual plies [20–22]. Validity of the macromechanics laminate model is evaluated by comparing with experimental results obtained. On accuracy of simulations, effects of strain rate dependence of apparent stiffness and a change in fiber orientation of plies induced by deformation [23–25] are also examined.

2. Materials and Testing Procedure

2.1. Materials and Specimens

Symmetrical alternating cross-ply carbon/epoxy laminates with a $[0/90]_{3S}$ lay-up were manufactured by the autoclave forming technique. The curing temperature was 130°C. The prepreg tape P2053F-20 (Toray) made of carbon fiber T800H and thermosetting epoxy resin #2500 was used.

Plain coupon specimens were cut from 400 mm by 400 mm cross-ply laminate panels. From the cross-ply laminate panels, five kinds of plain coupon specimens with different fiber orientations $\theta = 0, 5, 15, 45$ and $90°$ were cut. The off-axis angle θ represents the fiber orientation of the surface plies relative to the longitudinal direction of the specimens, and those off-axis specimens can be designated by the laminate code $[\theta/(90-\theta)]_{3S}$; in the following discussion, however, they are referred to by the off-axis angle θ for short. The shape and dimensions of the specimens are based on the testing standards JIS K7073 [26] and ASTM D3039 [27]; as shown in Fig. 1, the specimen length $L = 200$ mm, the gauge length $L_G = 100$ mm, the width $W = 20$ mm, and the thickness $t = 2$ mm, respectively. Rectangular-shaped

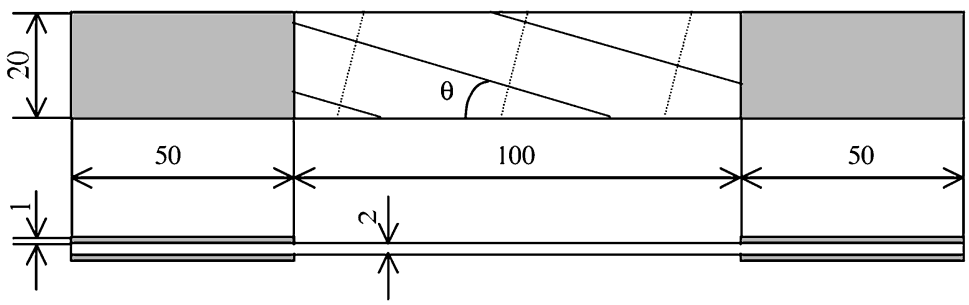

Figure 1. Specimen geometry (dimensions in mm).

aluminum-alloy tabs were attached on both ends of specimens using epoxy adhesive (Araldite); the thickness of the end-tabs was 1.0 mm. To obtain ample adhesive strength, the end tabs were bonded at 90°C in the oven (Gravity oven LG-112, Espec); specimens were exposed to the temperature for one hour.

2.2. Experimental Procedure

Constant strain-rate tests were carried out at two different strain rates of 1.0%/min (1.0 mm/min in the stroke rate) and 0.01%/min (0.01 mm/min), respectively, for each fiber orientation. Test temperature was specified to be a constant value of 100°C. Longitudinal and lateral strains of each specimen were monitored with two-element L-type rosette strain gauges. These strain gauges were mounted back-to-back at the center of each specimen.

Those static tension tests were performed using a servo-hydraulic MTS-810 testing machine of a dual servovalve type. The flow capacities of servovalves are 4 and 10 l/min, respectively. A heating chamber with a precise digital control capability (the maximum temperature is about 350°C) was employed for raising temperature of specimens. Specimens were heated up to 100°C in air without applying load, and preconditioned in the test environment for one hour prior to test; they were clamped in the heating chamber by the high temperature hydraulic wedge grips fitted on the testing machine. The variation of specimen temperature in time from the prescribed value was less than 1.0°C.

3. Experimental Results

The in-plane specimen coordinate system is denoted as (x, y), and the x-axis is taken in the loading direction. The principal axes of material anisotropy, i.e. the fiber coordinate system, for individual plies are expressed as $(1, 2)$; the 1-axis being in the fiber direction.

3.1. Off-Axis Stress–Strain Relationships

Axial stress–strain relationships ($\sigma_x - \varepsilon_x$) from tensile tests on the cross-ply T800H/2500 laminate specimens $[\theta/(90-\theta)]_{3S}$ at 100°C with constant strain rates of 1.0 and 0.01%/min are shown in Fig. 2(a) and 2(b), respectively, for all the fiber orientations θ. The on-axis stress–strain relationships ($\theta = 0$ and 90°) are almost linear and smooth until final failure. For the off-axis specimens with $\theta = 5$, 15 and 45°, by contrast, remarkable nonlinearity appears in the stress–strain relationships following the initial linear response. The nonlinearity of the shear stress–strain relationship was similar to that of the axial stress–strain relationship. These linear and nonlinear responses of the coupon specimens of the cross-ply laminate at 100°C are similar to those for unidirectional PMCs at the same test temperature [28]. Therefore, it is suggested that the nonlinearity of the off-axis tensile deformation of the cross-ply laminate is dominated by nonlinearity in shear deformation and it is similar to that of the unidirectional laminates made of the same prepreg tape. The

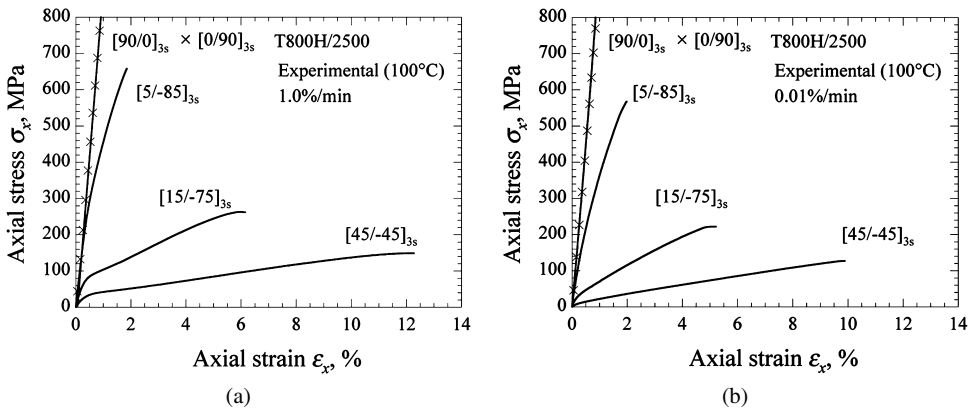

Figure 2. Off-axis stress–strain curves for the cross-ply T800H/2500 laminate at 100°C. (a) 1.0%/min; (b) 0.01%/min.

Table 1.
Engineering elastic components for the unidirectional T800H/2500 laminate at 100°C

E_1 (GPa)	E_2 (GPa)	G_{12} (GPa)	ν_{12}	ν_{21}
163.8	6.09	2.82	0.369	0.011

off-axis fracture strain was remarkably larger for $\theta = 45°$ in comparison with that for the other fiber orientations.

Inspecting the off-axis stress–strain curves for $\theta = 15$ and 45°, we notice that in the nonlinear regime the tangent modulus tends to increase slightly with increasing strain. This phenomenon may be ascribed to fiber rotation due to deformation of specimens [23–25]. A decrease in the ply orientation angle with extension leads to an increase in the apparent Young's modulus in the loading direction. The off-axis angle dependence of the initial value of the apparent Young's modulus, E_x, which is considered to be less influenced by fiber rotation, was accurately predicted using the classical laminated plate theory and the ply engineering elastic constants listed in Table 1. Table 2 shows comparisons between the predicted and observed apparent Young's moduli for all the fiber orientations.

3.2. Off-Axis Strain-Rate Dependence

The axial flow stress σ_x became smaller at a lower strain rate for all the off-axis fiber orientations, while no apparent influence of strain rate was observed for $\theta = 0$ and 90°. Comparisons between the off-axis stress–strain curves at 100°C for two different constant strain rates of 1.0%/min and 0.01%/min are shown in Fig. 3(a)–(c) for $\theta = 5$, 15 and 45°, respectively. The results at 1.0%/min are drawn in solid lines, and those at 0.01%/min in dashed lines. Comparing the axial flow

Table 2.
Off-axis Young's moduli for the cross-ply T800H/2500 laminate at 100°C

Θ (degree)	E_x (GPa)	
	Experimental	Predicted
0	82.6	85.3
5	69.8	70.4
15	29.2	30.9
45	11.2	10.6
90	81.6	85.3

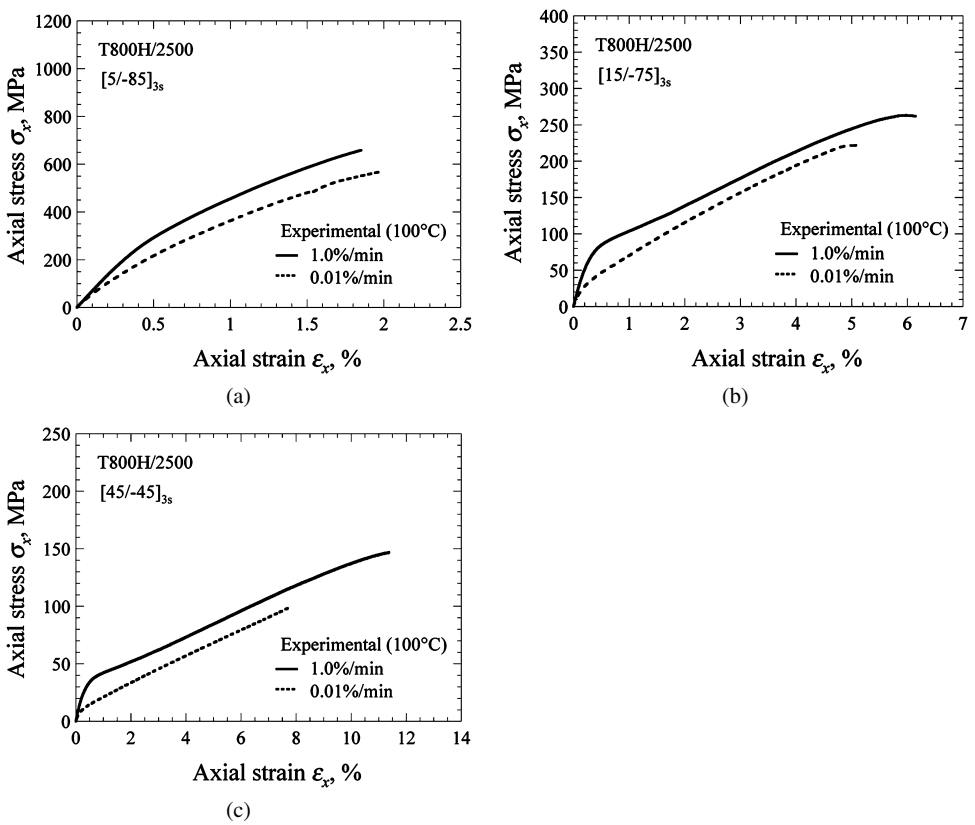

Figure 3. Rate dependence of the off-axis stress–strain curves for the cross-ply T800H/2500 laminate at 100°C under constant strain-rate conditions. (a) $[5/-85]_{3S}$; (b) $[15/-75]_{3S}$; (c) $[45/-45]_{3S}$.

stresses σ_x at the axial total strain of $\varepsilon_x = 1.0\%$, for example, we can see that the difference is about 21% ($\theta = 5°$), 34% (15°) and 53% (45°).

The shear stress–shear strain curve shown in Fig. 4 indicates that the shear flow stress associated with the lower strain rate became smaller by about 55% at the

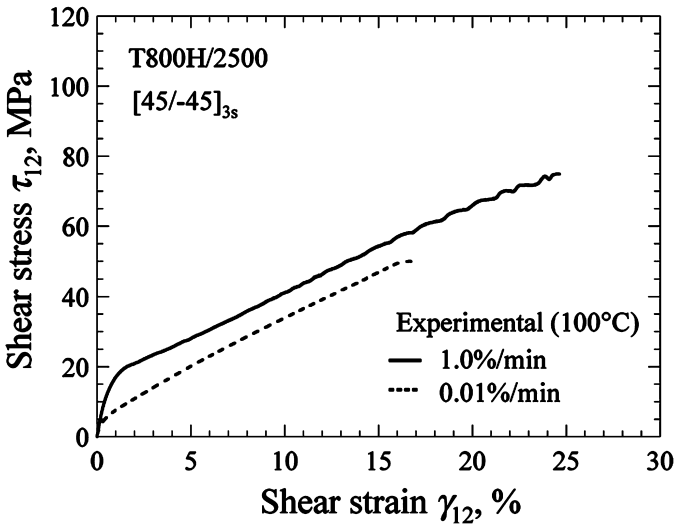

Figure 4. Rate dependence of the shear stress–strain curves for the cross-ply T800H/2500 laminate at 100°C under constant strain-rate conditions.

shear strain of $\gamma_{12} = 1.0\%$. Therefore, we can confirm that the rate dependence of the shear flow stress is comparable to that of the axial flow stress in the loading direction of the laminate, and the strain-rate dependence of the nonlinear off-axis deformation of the cross-ply laminate is closely related to the rate-dependent shear response of the epoxy resin employed.

The initial slope of the off-axis stress–strain curve became lower at the lower strain rate, except for $\theta = 0°$ and 90°. The reduction was about 22% for $\theta = 5°$, 34% for $\theta = 15°$ and 37% for $\theta = 45°$. The in-plane shear modulus G_{12} evaluated on the basis of the shear stress–strain relationship ($\theta = 45°$) was 1.55 GPa at the lower strain rate of 0.01%/min, and it was smaller by about 31% compared with the value of 2.25 GPa at the higher strain rate of 1.0%/min. Similar rate dependence of the initial apparent Young's modulus was observed for the off-axis nonlinear behavior of unidirectional CFRP laminates [28]. Therefore, it follows that the initial slope of the off-axis stress–strain curve also depends on the rate of deformation. It is believed that this phenomenon reflects the rate-dependent elastic response of the matrix resin, since polymer materials exhibit viscoelasticity over a wide range of temperature [4].

These experimental results suggest that not only the rate dependence of nonlinear deformation upon loading to a relatively high stress level but also the rate dependence of deformation in an apparently linear response in the range of small stress should appropriately be taken into account for accurate predictions of the overall nonlinear rate-dependent deformation behavior of the cross-ply laminate under off-axis loading conditions at high temperature.

4. Rate-Dependent Inelasticity Model for Laminates

A phenomenological viscoplasticity model for laminates is constructed using the classical laminated plate theory [18, 19] with a viscoplastic constitutive model for individual plies [20–22]. The ply viscoplasticity model assumed in the present formulation is based on the overstress concept as well as the effective stress and inelastic strain proposed by Sun and Chen [14] and Ha and Springer [29].

The mechanical strain of plies may involve a linear/nonlinear viscoelasticity contribution, as reflected by the moderate rate dependence of the initial slope of the axial stress–strain relationship under off-axis loading. This phenomenon is described using only a very simple model in this study, since no ample data are available for accurately separating a total strain into viscoelastic and viscoplastic components.

Applying a high stress or a large strain to polymers reactivates their physical aging. This implies that the creep behavior of PMCs at relatively high stress levels is influenced by the aging-induced property change of the polymer matrix employed. Presently, no ample data for modeling the relevant time hardening/softening behavior of PMCs are available. Therefore, the material constants appearing in the ply models were determined to fit the basic experimental data on unidirectional laminates involving the effects of physical aging.

4.1. A Viscoplasticity Model for Laminates

Using the classical lamination theory [18, 19] together with a viscoplasticity model for individual plies, we can write the constitutive equation for the in-plane deformation of a symmetric laminate in the following rate form:

$$\dot{\boldsymbol{\sigma}}^0 = \mathbf{A}^*(\dot{\boldsymbol{\varepsilon}}^0 - \dot{\boldsymbol{\varepsilon}}^p), \tag{1}$$

where $\dot{\boldsymbol{\sigma}}^0$ and $\dot{\boldsymbol{\varepsilon}}^0$ denote the average stress rate and the midplane total strain rate of the laminate, respectively. The second term $\dot{\boldsymbol{\varepsilon}}^p$ in the parentheses represents the average viscoplastic strain rate of the laminate, and it can be expressed as

$$\dot{\boldsymbol{\varepsilon}}^p \equiv \mathbf{A}^{-1} \sum_k t_k \overline{\mathbf{Q}^{(k)}}\, \overline{\dot{\boldsymbol{\varepsilon}}^{p(k)}}, \tag{2}$$

where $\mathbf{A}$ is the extensional stiffness of the laminate, and it is defined as

$$\mathbf{A} \equiv \sum_k t_k \overline{\mathbf{Q}^{(k)}}. \tag{3}$$

The quantities $\overline{\mathbf{Q}^{(k)}}$, $\overline{\dot{\boldsymbol{\varepsilon}}^{p(k)}}$ and t_k represent the transformed stiffness, viscoplastic strain rate, and thickness of the kth ply, respectively. The matrix $\mathbf{A}^*$ in equation (1) stands for the effective extensional stiffness defined as $\mathbf{A}/t$ in which $t = \sum t_k$.

The stress rate in the kth ply is expressed as

$$\overline{\dot{\boldsymbol{\sigma}}^{(k)}} = \overline{\mathbf{Q}^{(k)}}\left(\dot{\boldsymbol{\varepsilon}}^0 - \overline{\dot{\boldsymbol{\varepsilon}}^{p(k)}}\right). \tag{4}$$

All barred quantities have the components in the specimen coordinate system. The off-axis components of $\overline{\dot{\boldsymbol{\varepsilon}}^{p(k)}}$ in equations (2) and (4) are obtained from the in-plane coordinate transformation of the components of $\dot{\boldsymbol{\varepsilon}}^{p(k)}$ in the fiber coordinate system. Note that the averaged quantities $\dot{\boldsymbol{\sigma}}^0$, $\dot{\boldsymbol{\varepsilon}}^0$ and $\dot{\mathbf{e}}^p$ have the components in the specimen coordinate system, though they are not barred.

4.2. A Viscoplasticity Model for Plies

In phenomenological viscoplasticity formulations for engineering materials, an effective viscoplastic strain rate $\bar{\dot{\varepsilon}}^p$ is typically expressed in the form

$$\bar{\dot{\varepsilon}}^p = \left\langle \frac{H}{K} \right\rangle^{1/m}, \tag{5}$$

where H stands for an effective overstress, and K and m are material constants. The angular brackets in equation (5) denote the function: $\langle x \rangle = \max\{x, -x\} = x(x \geqslant 0) = 0(x < 0)$. The effective overstress H represents the magnitude of a net stress that determines the magnitude of viscoplastic strain rate.

A simple form of the effective overstress can be given as

$$H \equiv \bar{\sigma} - r, \tag{6}$$

where $\bar{\sigma}$ is an effective stress, and r is a scalar hardening variable to describe the time- and rate-dependent nonlinear behavior.

To obtain a concrete form of the viscoplasticity model for unidirectional plies under plane stress conditions, we adopt the following expressions of the effective stress and effective viscoplastic strain rate [14]:

$$\bar{\sigma} = \sqrt{\frac{3}{2}\left(\sigma_{22}^2 + 2a_{66}\sigma_{12}^2\right)}, \tag{7}$$

$$\bar{\dot{\varepsilon}}^p = \sqrt{\frac{2}{3}\left(\dot{\varepsilon}_{22}^{p2} + \frac{1}{2a_{66}}\dot{\gamma}_{12}^{p2}\right)}, \tag{8}$$

where a_{66} is a material constant. Note that equations (7) and (8) are defined using the stress and strain components in the principal axes of material anisotropy.

As implied by equations (7) and (8), it is postulated that no inelastic strain appears in the fiber direction of unidirectional plies. Thus, the inelastic strain rate in individual plies can be expressed as

$$\begin{Bmatrix} \dot{\varepsilon}_{11}^p \\ \dot{\varepsilon}_{22}^p \\ \dot{\gamma}_{12}^p \end{Bmatrix} = \frac{3}{2}\frac{\bar{\dot{\varepsilon}}^p}{\bar{\sigma}} \begin{bmatrix} 0 & 0 & 0 \\ 0 & 1 & 0 \\ 0 & 0 & 2a_{66} \end{bmatrix} \begin{Bmatrix} \sigma_{11} \\ \sigma_{22} \\ \sigma_{12} \end{Bmatrix} \tag{9}$$

in the fiber coordinate system.

The evolution equation of the scalar internal variable r is represented as

$$\dot{r} = \sum_i \dot{r}_i = \sum_i b_i(Q_i - r_i)\bar{\dot{\varepsilon}}^p, \tag{10}$$

where Q_i's stand for the saturated values of r_i, and material constants b_i characterize the manner in which r_i's approach their saturated values. Such a superposition of the same type of internal variables with different nonlinearities is useful for enhancing the accuracy of the model to describe the nonlinear response of materials [30].

4.3. Rate-Dependent Stiffness

The ply viscoplasticity model described above cannot describe the rate dependence of the initial slope of the off-axis stress–strain relationship. In this study, a limited approach to solve this problem is adopted, in which the time dependence of compliance is assumed. The rate form of the Hooke's law can then be given in the following form:

$$\begin{Bmatrix} \dot{\varepsilon}^e_{11} \\ \dot{\varepsilon}^e_{22} \\ \dot{\gamma}^e_{12} \end{Bmatrix} = \begin{bmatrix} S_{11} & S_{12} & 0 \\ S_{12} & S_{22}(t) & 0 \\ 0 & 0 & S_{66}(t) \end{bmatrix} \begin{Bmatrix} \dot{\sigma}_{11} \\ \dot{\sigma}_{22} \\ \dot{\tau}_{12} \end{Bmatrix} + \begin{bmatrix} 0 & 0 & 0 \\ 0 & \dot{S}_{22}(t) & 0 \\ 0 & 0 & \dot{S}_{66}(t) \end{bmatrix} \begin{Bmatrix} \sigma_{11} \\ \sigma_{22} \\ \tau_{12} \end{Bmatrix}, \tag{11}$$

where only the transverse and shear components of the compliance matrix are assumed to be time-dependent.

5. Simulations

5.1. Material Identification

In the present study, the scalar internal variable r was prescribed by the sum of three components r_i $(i = 1, 2, 3)$ that grow with different nonlinearities. Hence, the number of material constants involved by the ply viscoplasticity model comes to nine in total; K, m, Q_i, b_i and a_{66}. These material constants were determined on the basis of the off-axis tensile behavior of the unidirectional laminate made of the same kind of prepreg tapes, following the procedure described in [16, 17], and they were finally identified as listed in Table 3. The reference engineering elastic constants of the constituent plies were evaluated from the off-axis tension test results on the unidirectional laminates at the constant strain rate of 1.0%/min, and they are listed in Table 1.

Table 3.
Material parameters for the ply viscoplasticity model

α_{66}	Q_1 (MPa)	Q_2 (MPa)	Q_3 (MPa)	b_1	b_2	b_3	K ($\mathrm{MPa^m\ min^m}$)	m
2.0	18	110	13	400	20	10000	46.4	0.29

The compliance functions to describe the rate dependence of the initial slope of the off-axis stress–strain relationship are specified as

$$S_{22}(t) = A_2 - B_2 \exp(-C_2 t), \tag{12}$$

$$S_{66}(t) = A_6 - B_6 \exp(-C_6 t), \tag{13}$$

where the coefficients A_2, B_2, C_2 were determined on the basis of the rate dependence of the initial slope for $\theta = 90°$, and the coefficients A_6, B_6 and C_6 determined so as to obtain better predictions of the initial slopes of the shear stress–strain curves which were extracted from the results on the 45° specimens for the loading at different strain rates. These coefficients were finally identified as listed in Table 4.

The predicted off-axis stress–strain relationships for the unidirectional CFRP laminate at 100°C for the constant strain rate of 1.0%/min are shown in Fig. 5, together with the experimental results. Good agreements between the calculated and observed results have been achieved in both the initial linear and the subsequent nonlinear regimes. Figure 6 shows comparisons between the predicted and experimental shear stress–shear strain relationships for different stress rates of 1.0,

Table 4.
Material parameters for the ply viscoelasticity model

A_2 (MPa^{-1})	B_2 (MPa^{-1})	C_2 (min^{-1})	A_6 (MPa^{-1})	B_6 (MPa^{-1})	C_6 (min^{-1})
2.0×10^{-4}	5.7×10^{-5}	10	6.5×10^{-4}	3.1×10^{-4}	10

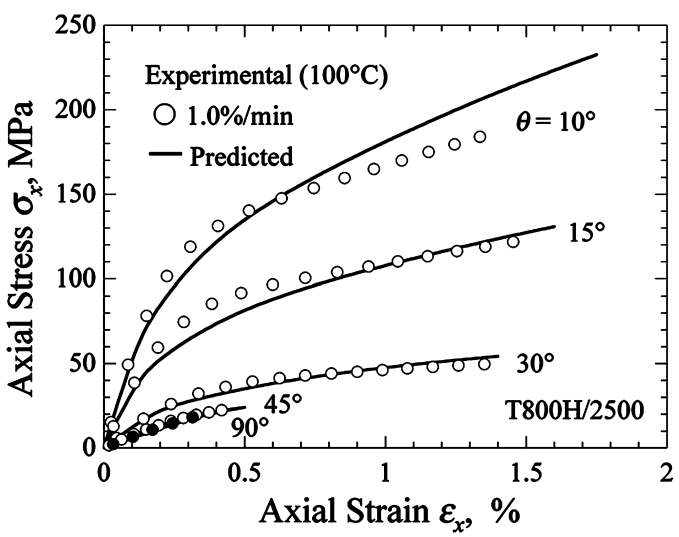

Figure 5. Predicted off-axis stress–strain curves for the unidirectional T800H/2500 laminate at 1.0%/min.

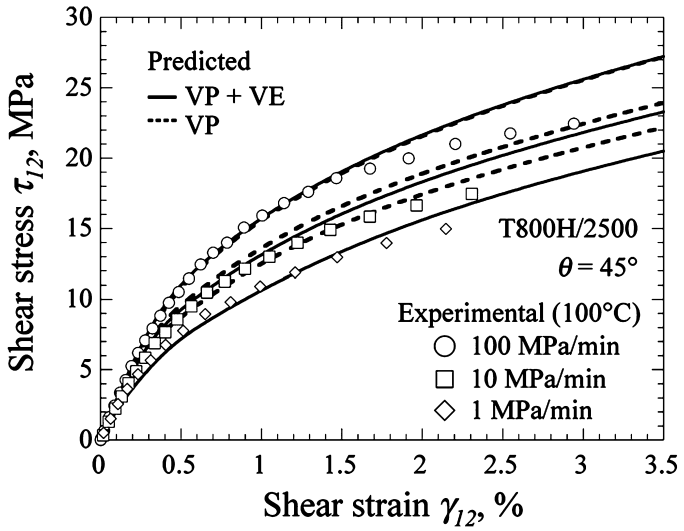

Figure 6. Predicted rate-dependent shear stress–shear strain curves for $\theta = 45°$ under constant stress-rate conditions.

10 and 100 MPa/min, respectively; these experimental data had been obtained earlier in [28]. It is noticeable that the strain-rate effect on the nonlinear stress–strain curves are more adequately described using the viscoplastic–viscoelastic laminate model (VP + VE) over the tested range of strain, when compared with the simulation results without considering viscoelasticity (VP). The reasonable agreements observed in Figs 5 and 6 prove the validity of the material constants identified.

5.2. Comparisons With Experimental Results

The predicted stress–strain curves of the cross-ply laminate specimens are shown in Fig. 7 by dashed lines for the off-axis fiber orientations $\theta = 5$, 15 and 45°, together with the experimental results. It is seen that the predictions agree well with the experimental results in the range of small strain. However, the predicted axial flow stress tends to become smaller than the experimental result with increasing strain.

Such underestimation of the axial flow stress in a large strain range is ascribed to the relative fiber rotation due to the overall extensional deformation of the laminate. A decrease in the fiber orientation angle of ply brings about an increase in the extensional stiffness of the laminate in the loading direction. Assuming a uniform lateral contraction of the cross-ply laminate specimen upon in-plane off-axis tensile loading and a uniform shear coupling effect, we can evaluate the deformation-induced fiber orientation change by means of the following formula:

$$\theta' = \arctan\left(\alpha \frac{1+\varepsilon_y^0}{(1+\varepsilon_x^0)/\tan\theta + (1+\varepsilon_y^0)/|\tan\gamma_{xy}^0|}\right), \tag{14}$$

where θ and θ' stand for the fiber orientation angles before and after tensile deformation, respectively. The effect of inhomogeneous deformation of the gauge–length

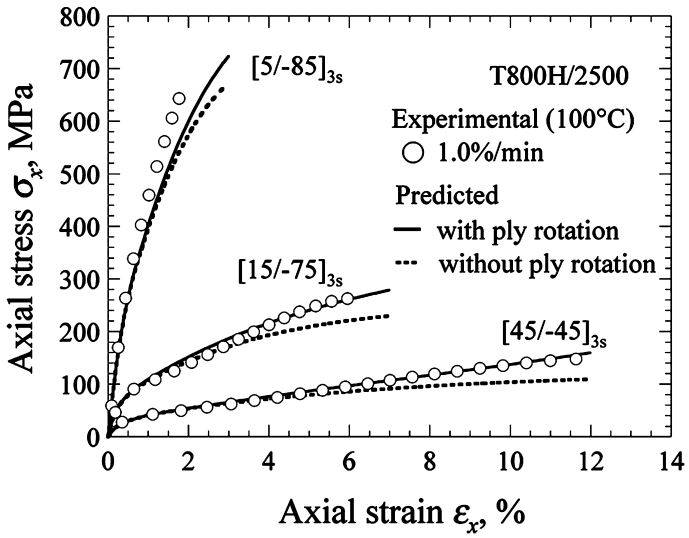

Figure 7. Predicted off-axis stress–strain curves for the cross-ply T800H/2500 laminate at 1.0%/min.

part of actual specimens is considered in the present analytical evaluations by including an adjusting factor α in the round brackets of equation (14); it may be assumed that the factor has the value of unity in the case of numerical evaluations of finite deformation using FEM.

The solid lines in Fig. 7 indicate the simulation results obtained by considering the deformation-induced fiber orientation change. In those calculations, the adjusting factor was specified as $\alpha = 1.0$ for $\theta = 5$ and 15°, and $\alpha = 1.03$ for $\theta = 45°$. We can see that the predictions considering fiber rotation agree well with the experimental results over the whole range of strain up to ultimate failure.

Figure 8(a)–(c) shows comparisons between the predicted and observed rate-dependent deformation behaviors for the off-axis fiber orientations $\theta = 5$, 15 and 45°, respectively. The solid lines in these figures represent the calculations that have considered the deformation-induced fiber rotation as well as the viscoelastic deformation of plies, and they agree well with the experimental results over the whole range of strain in comparison with the dashed lines that indicate the results obtained by considering only fiber rotation. This reveals that consideration of the rate dependence of the initial stiffness slightly improves the accuracy of predictions. Therefore, it may be concluded that the rate-dependent nonlinear behavior of the cross-ply laminate under off-axis loading conditions can adequately be predicted using the phenomenological laminate model based on the classical lamination theory and the ply viscoelastoplasticity model.

Good predictions were obtained in the present study in spite of disregarding the effect of damage. This is partly because the material constants of the ply viscoplasticity model have been identified on the basis of the off-axis inelastic behavior of the unidirectional laminate that is accompanied with damage. To develop a more

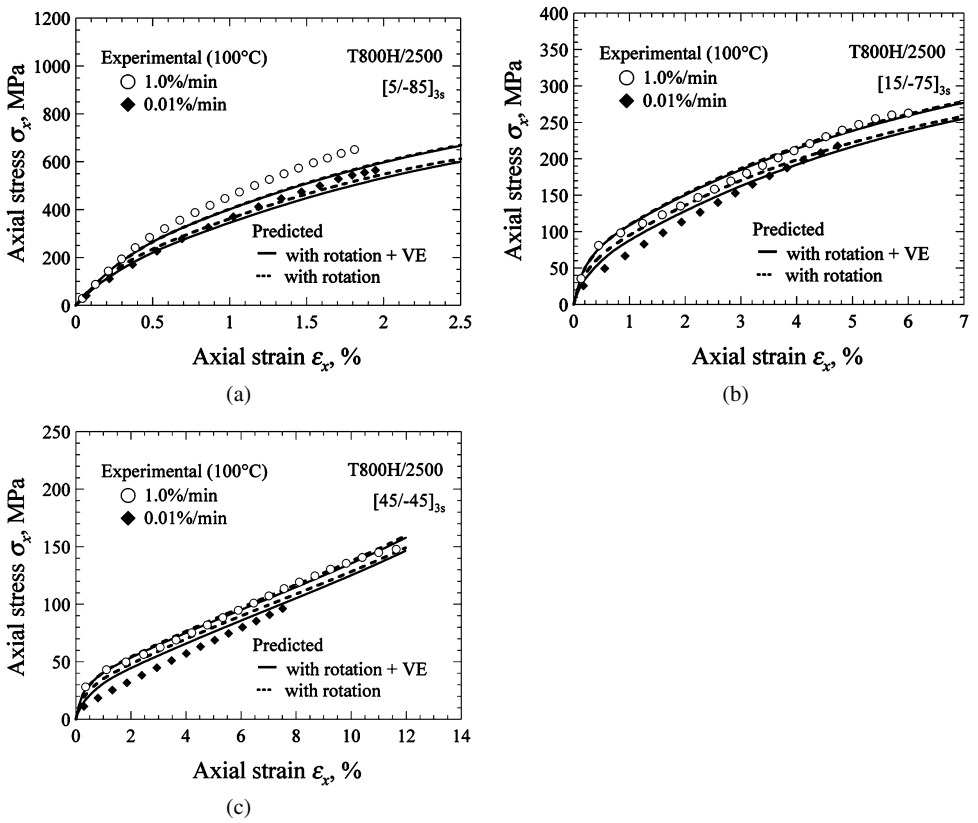

Figure 8. Predicted rate-dependent off-axis stress–strain curves for the cross-ply T800H/2500 laminate under constant strain-rate conditions. (a) $[5/-85]_{3S}$; (b) $[15/-75]_{3S}$; (c) $[45/-45]_{3S}$.

physically-based model, a progress of damage in laminates should be considered as well. The quest for further sophistication is however left for future studies that accompany more detailed information on the inelastic behavior of plies and laminates under nonmonotonic complicated loading conditions.

6. Conclusions

The strain-rate dependence of the off-axis deformation behavior of the symmetric cross-ply T800H/2500 carbon/epoxy laminate at 100°C was examined. A ply-by-ply basis inelastic analysis was performed using the macromechanical constitutive model based on the classical laminated plate theory and a combined viscoelasticity and viscoplasticity model for unidirectional plies. Effects of fiber rotation of plies due to large deformation were also considered in the simulations of the cross-ply laminate. Validity of the CLT-based viscoelastoplasticity model was evaluated by comparing with experimental results. The major results in this work can be summarized as follows:

(1) Significant nonlinearity appears in the stress–strain relationship of the cross-ply laminate under off-axis loading at high temperature. The axial flow stress in the range of nonlinear deformation depends on the rate of deformation, and it becomes smaller at a lower strain rate. The extent of the rate dependence of the off-axis flow stress is comparable with that of the in-plane shear flow stress, suggesting that the overall rate dependence is controlled by the rate-dependent plastic flow of the epoxy matrix.

(2) The initial slope of the off-axis stress–strain relationship of the cross-ply laminate also exhibits moderate rate dependence, and it becomes milder at a lower strain rate except for loading in the fiber directions. This reflects the inherent viscoelasticity of the epoxy matrix.

(3) A simple viscoelastoplasticity model has been formulated which can describe the rate dependence of the initial linear response as well as the subsequent nonlinear response of unidirectional laminates under off-axis loading. A ply-by-ply basis laminate inelasticity model for multidirectional laminates has also been developed on the basis of the classical lamination theory and the viscoelastoplasticity model for individual plies.

(4) The nonlinearity and rate dependence of the tensile deformation of the symmetric alternating cross-ply laminate under off-axis loading at 100°C are successfully predicted using the proposed ply-by-ply basis laminate inelasticity model with a consideration of the deformation-induced fiber rotation of plies.

Acknowledgement

The authors are grateful to Dr. Y. Masuko for his assistance of testing and material identification.

References

1. L. H. V. Vlack, *Materials Science for Engineers*. Addison-Wesley, MA, USA (1970).
2. C. R. Barrett, W. D. Nix and A. S. Tetelman, *The Principles of Engineering Materials*. Prentice-Hall, Englewood Cliffs, UK (1973).
3. T. H. Courtney, *Mechanical Behavior of Materials*. McGraw-Hill, Singapore (1990).
4. S. Matsuoka, *Relaxation Phenomena in Polymers*. Oxford University Press, New York, USA (1992).
5. L. E. Nielsen, *Mechanical Properties of Polymers and Composites*. Marcel Dekker, New York, USA (1975).
6. W. H. Morita and S. R. Graves, Graphite/polyimide technology overview and space shuttle orbiter applications, in: *Proc. 14th National SAMPE Technical Conference*, October 12–14, pp. 387–401 (1982).
7. J. S. Jones, Celion/Larc-160 graphite/polyimide composite processing techniques and properties, in: *Proc. 14th National SAMPE Technical Conference*, October 12–14, pp. 402–417 (1982).

8. T. S. Gates and C. T. Sun, Elastic/viscoplastic constitutive model for fiber reinforced thermoplastic composites, *AIAA Journal* **29**, 457–463 (1991).
9. M. Kawai, Y. Masuko, Y. Kawase and R. Negishi, Micromechanical analysis of the off-axis rate-dependent inelastic behavior of unidirectional AS4/PEEK at high temperature, *Int. J. Mech. Sci.* **43**, 2069–2090 (2001).
10. C. T. Sun and K. J. Yoon, Characterization of elastic–plastic behavior of AS4/PEEK thermoplastic composite for temperature variation, *J. Compos. Mater.* **25**, 1297–1313 (1991).
11. K. J. Yoon and C. T. Sun, Characterization of elastic–plastic behavior of an AS4/PEEK thermoplastic composite, *J. Compos. Mater.* **25**, 1277–1296 (1991).
12. C. Wang and C. T. Sun, Experimental characterization of constitutive models for PEEK thermoplastic composite at heating stage during forming, *J. Compos. Mater.* **31**, 1480–1506 (1997).
13. P. Ladeveze and E. L. Dantec, Damage modelling of the elementary ply for laminated composites, *Compos. Sci. Technol.* **43**, 257–267 (1992).
14. C. T. Sun and J. L. Chen, A simple flow rule for characterizing nonlinear behavior of fiber composites, *J. Compos. Mater.* **23**, 1009–1020 (1989).
15. S. R. Bodner and Y. Partom, Constitutive equations for elastic–viscoplastic strain-hardening materials, *ASME J. Appl. Mech.* **42**, 385–389 (1975).
16. Y. Masuko and M. Kawai, Application of a phenomenological viscoplasticity model to the stress relaxation behavior of unidirectional and angle-ply CFRP laminates at high temperature, *Composites, Part A* **35**, 817–826 (2004).
17. M. Kawai and Y. Masuko, Creep behavior of unidirectional and angle-ply T800H/3631 laminates at high temperature and simulation using a phenomenological viscoplasticity model, *Compos. Sci. Technol.* **64**, 2373–2384 (2004).
18. S. W. Tsai and H. T. Hahn, *Introduction to Composite Materials*. Technomic Publishing Co, Lancaster, PA (1980).
19. D. Hull, *Introduction to Composite Materials*. Cambridge University Press, UK (1982).
20. M. Kawai, A phenomenological constitutive model for metal matrix composites, in: *Proc. Int. Seminar on Microstructures and Mechanical Properties of New Engineering Materials*, M. Tokuda, B. Xu and M. Senoo (Eds), pp. 599–606. Mie Academic Press, Tsu, Japan (1993).
21. M. Kawai, Constitutive model for non-linear behavior of unidirectionally fiber reinforced metal matrix composites, in: *Advances in Engineering Plasticity and Its Applications*, B. Xu and W. Yang (Eds), pp. 95–100. International Academic Publishers, Beijing, China (1994).
22. M. Kawai and Y. Masuko, Macromechanical modeling and analysis of the viscoplastic behavior of unidirectional fiber-reinforced composites, *J. Compos. Mater.* **37**, 1885–1902 (2003).
23. M. R. Wisnom, The effect of fibre rotation in $\pm 45^\circ$ tension tests on measured shear properties, *Composites, Part A* **26**, 25–32 (1995).
24. C. T. Herakovich, R. D. Schroedter III, A. Grasser and L. Guitard, Damage evolution in $[\pm 45]_s$ laminates with fiber rotation, *Compos. Sci. Technol.* **60**, 2781–2789 (2000).
25. C. T. Sun and C. Zhu, The effect of deformation-induced change of fiber orientation on the nonlinear behavior of polymeric composite laminates, *Compos. Sci. Technol.* **60**, 2337–2345 (2000).
26. JIS K7073, Testing method for tensile properties of carbon fiber-reinforced plastics, Japanese Industrial Standard. Japanese Standards Association (1988).
27. ASTM D3039, Standard test method for tensile properties of fiber–resin composites. ASTM Standards and Literature References for Composite Materials, ASTM (1987).
28. M. Kawai, Y. Masuko and M. Kohashi, Rate dependence of linear and nonlinear behaviors of unidirectional CFRP under off-axis loading at high temperature, *Japan. Int. SAMPE, JISSE7*, Tokyo Big Sight, November 13–16, pp. 849–852 (2001).

29. S. K. Ha and G. S. Springer, Time dependent behavior of laminated composite at elevated temperature, *J. Compos. Mater.* **23**, 1159–1197 (1989).
30. J. L. Chaboche, Viscoplastic Constitutive equations for the description of cyclic and anisotropic behavior of metals, *Bulletin de L'Academie Polonaise des Science, Série de Science Techniques* **25**, 33–42 (1977).